ISSN: 2710-0588

Thermal and Structural Performance Analysis of Piezoelectric Acceleration Sensor

Chuanqing Pang, Zhi Qiu, Fayi Liao

School of Mechanical and Electrical Engineering, Southwest Petroleum University, Chengdu 610500, China

Abstract

Thermal and structural piezoelectric acceleration sensors are complicated and affected by many factors, especially when the sensor works in different temperature environments, its performance and structure will be affected to some extent. In this paper, the interference contact model of piezoelectric sensor is established with the method of bolt preloading, and the finite element analysis is carried out under different interference quantities. Moreover, based on the bolt preload model, the loading method of temperature load is studied, and the structural thermal adaptation characteristics of the sensor under the conditions of -70℃, -50℃, 0℃, 120℃, 160℃ and 200℃ are analyzed. Based on these thermal deformation and thermal stress analysis at different temperatures, the thermal adaptation characteristics of the sensor are analyzed. The normal operating temperature range of the sensor is -50℃ -120 ℃, and the structural parameter of the sensor (the thickness of the base) is optimized, so that the operating temperature of the sensor can reach 200℃. Ability to analyze.

Keywords

Piezoelectric Sensor; Workbench Finite Element Analysis; Thermal - Structural Coupling Analysis.

1. Introduction

High temperature acceleration sensor is a key instrument and equipment, widely used in aerospace, energy, transportation and other fields [1]. With the continuous development of science and technology and the improvement of performance stability requirements in higher temperature environments, it is particularly important for researchers to analyze and optimize the structural thermal stability of high temperature acceleration sensors. In high temperature environment, the stability of the acceleration sensor structure is very important for the measurement accuracy and long-term reliable operation. The sensor structure is affected by thermal expansion, thermal stress, heat release and other factors in high temperature environment, which may lead to degradation, failure or destruction of sensor performance, thus affecting the normal operation of the whole system [2]. Therefore, it is of great significance to study the thermal stability of the acceleration sensor structure in high temperature environment to improve its working efficiency and extend its service life [3].

At present, there are relatively few researches on the structural thermal stability of acceleration sensors in high temperature environment. The existing researches mainly focus on the analysis of the influence of parameters such as temperature and thermal expansion coefficient on the performance of sensors [4], and there are still some deficiencies in the research on the optimization design of the stability of sensor structures under high temperature environment. Therefore, it is necessary to deeply explore the thermal stability of high temperature acceleration sensor structure, and put forward corresponding solutions to meet the needs of the acceleration sensor under high temperature conditions.

ISSN: 2710-0588

The purpose of this paper is to improve the reliability and performance stability of high temperature acceleration sensor by analyzing and optimizing the structural thermal stability. Specifically, starting from material selection and structural design, we will study key issues such as thermal stress distribution and deformation of acceleration sensor structure in high temperature environment through finite element simulation [5]. At the same time, the corresponding improvement scheme and optimization strategy are proposed to improve the thermal stability of the sensor structure and meet the needs of engineering applications.

2. Structure and Principle of Piezoelectric Acceleration Sensor

2.1. Principles and Piezoelectric Effects

When the piezoelectric material forces it in a specific direction, the deformation inside the crystal, the release of electric charges, and the electrodes on both sides of the material change. When the external force disappears, the charge also disappears, so the electrical conversion of the piezoelectric material has an elastic and reversible force. If the direction of the external force is changed, the polarity of the generated charge will also change.

The piezoelectric effect is a reaction to the elastic properties of piezoelectric materials and to the mechanical properties of electrons. The two characteristics of the piezoelectric effect are the inverse piezoelectric effect and the positive piezoelectric effect. If pressure is applied to the piezoelectric material, a certain charge will be released at both ends of the material. On a piezoelectric material, if we apply an external electric field, its crystal will become polarized and it will experience stress and strain [6].

When the external forces normally applied to the piezoelectric material are reduced, the piezoelectric effect and the reverse piezoelectric effect are to some extent linear mathematical and produce dielectric effects that are linearly dependent on the pressure. When an external electric field is applied to a piezoelectric material, the stress generated is linearly related to the deformation and resistance of the external electric field. Therefore, piezoelectric materials with linear elasticity are suitable for simulating linear structural analysis, so this is often used in finite element analysis.

When the piezoelectric material is subjected to external stress, it will produce its piezoelectric effect, which can be expressed by the following formula:

$$\begin{pmatrix} p_1 \\ p_2 \\ p_3 \end{pmatrix} = \begin{pmatrix} k_{11} & k_{12} & k_{13} & k_{14} & k_{15} \\ k_{21} & k_{22} & k_{23} & k_{24} & k_{25} \\ k_{31} & k_{32} & k_{33} & k_{34} & k_{35} \end{pmatrix} \begin{pmatrix} \alpha_1 \\ \alpha_2 \\ \alpha_3 \\ \alpha_4 \\ \alpha_5 \\ \alpha_6 \end{pmatrix} \tag{1}$$

Where: P-the density of charge generated outside the piezoelectric material.

a-Stress on a piezoelectric material.

K-piezoelectric constant.

2.2. Piezoelectric Acceleration Sensor Structure

The basic structure of the piezoelectric acceleration sensor includes a mass block, a piezoelectric sensing element and a base. These components are usually pre-tightened with

ISSN: 2710-0588

bolts, but can also be secured by other means, such as binder or inorganic adhesive. In order to isolate external power frequency noise, it is usually equipped with a housing. The amount of induced charge in piezoelectric acceleration sensors is very small, so measures need to be taken to protect and derive the charge. Piezoelectric sensors are usually not electrically conductive, so the charge needs to be derived using conductive sheets, etc., and connected to the subsequent processing part through wires.

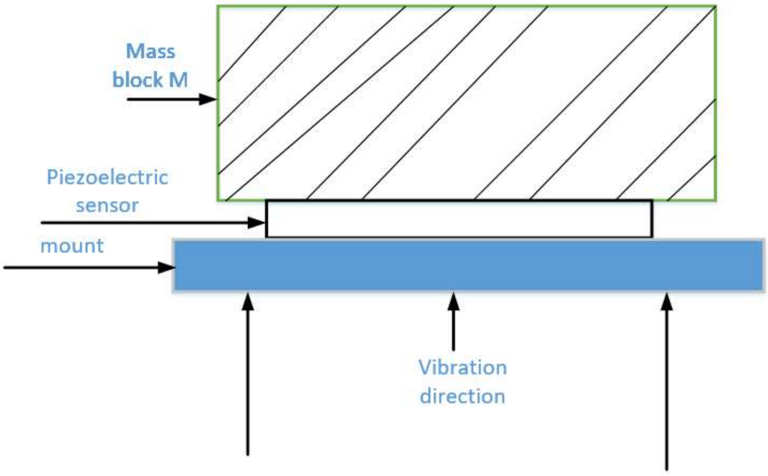

Figure 1. Schematic diagram of a piezoelectric acceleration sensor

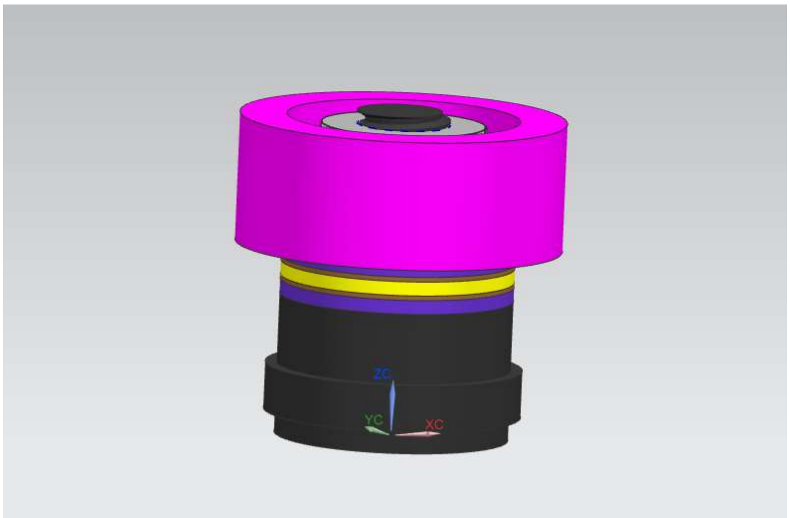

Figure 2. UG model of a sensor

2.3. Interference Preloading Method

Interference preloading method when determining the interference problem, the reality is that the bolt is connected to the connected piece, the bolt will extend, the connected piece compression, the interference amount is determined by these two factors. In the interference preloading method, in order to simplify the model, the extension of the bolt is usually considered unilaterally to replace the interference, so the formula is obtained:

$$\Delta L = \frac{F_0 L}{\pi d^2 E} \tag{2}$$

ISSN: 2710-0588

Where:
F_0-preload.
L-bolt original clamping length.
E-Elastic modulus of the bolt corresponding to the material.
d-the path of the bolt.

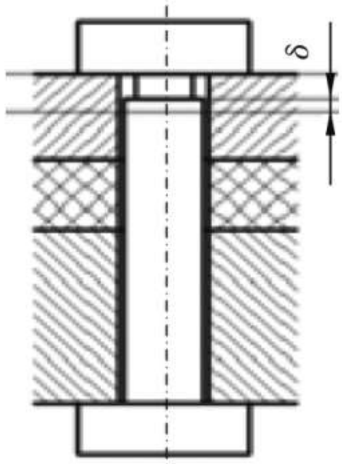

Figure 3. Bolt elongation diagram

Assuming that the connected part is a rigid body, then:

$$\mathrm{M}_t = \frac{KP_0}{1000d} \tag{3}$$

$$\sigma_0 = \frac{P_0}{A_s} \tag{4}$$

$$\sigma_0 = (0.5\sim0.7)\sigma_s \tag{5}$$

Where:
K-tightening force coefficient.
P_0- tightening force.
d-nominal diameter of thread.
A_s- dangerous cross section area.
σ_s- the yield limit of a material.
Bring in the corresponding parameter: d=4mm, K=0.19, $A_s = 8.8mm^2$, $\sigma_s = 300MPa, L = 14mm$,$\mathrm{E} = 2.06 \times 10^5 N/mm^2$.
Assume that the installation torque M_t is in three cases: 1N/m, 1.5N/m, 2N/m, Can be obtained by formula (3)(4) (5):
When M_t=1N/m, F_0=1315N, ΔL=0.002mm.
When M_t=1.5N/m, F_0=1973N, ΔL=0.00286mm.
When M_t=2N/m, F_0=2632N, ΔL=0.00381mm.

ISSN: 2710-0588

3. Finite Element Analysis of Sensor with Different Interference Volume under ANSYS

3.1. ANSYS Simulation Software Introduction

ANSYS is a powerful finite element analysis software developed by the American ANSYS company. It integrates a variety of simulation scenarios and provides a simple and easy-to-use operating interface via ANSYS Workbench. ANSYS is widely used in the analysis of structure, fluid, electric field, magnetic field, sound field and so on. In the structural dynamics analysis, ANSYS can carry out modal analysis, transient dynamics analysis and harmonic response analysis. Modal analysis is used to determine the natural frequency and mode of the structure, transient dynamic analysis is used to simulate the response of the structure in time, and harmonic response analysis is used to evaluate the response of the structure under harmonic excitation. In addition, ANSYS provides a wealth of post-processing capabilities for visual analysis of results.

3.2. Selection of Finite Element Analysis Method for Piezoelectric Sensor

In general, piezoelectric sensor structures have an initial state of the bolt before tightening. The analysis of the preload force includes the finite element analysis of the structure, and the preload state of the bolt is the basic state of the whole sensor. The basic state is the constant operating state of the inactive state. In order to analyze the static preload of the sensor, an ANSYS module for structural analysis is required, which can simply be called bolt preload analysis at room temperature.

3.3. Performance Analysis of Piezoelectric Sensors with Different Interference Quantities

3.3.1. Interference Magnitude 0.0020mm Stress Displacement Analysis

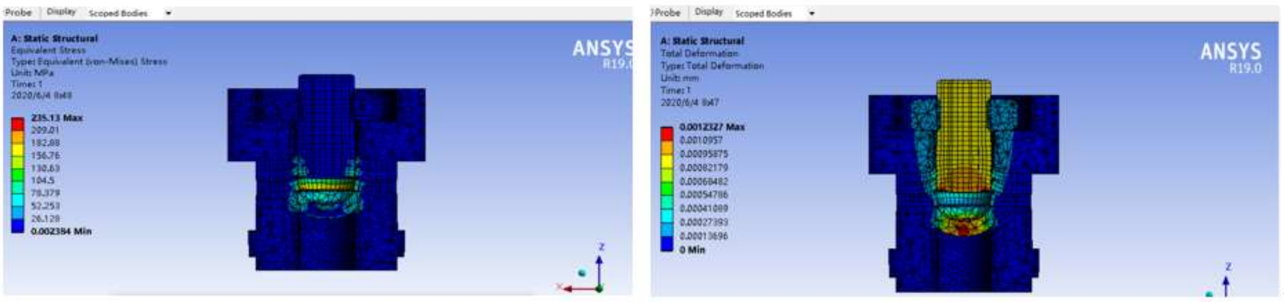

Figure 4. Interference magnitude 0.0020mm sensor stress-strain distribution

3.3.2. Interference Magnitude 0.0028mm Stress Displacement Analysis

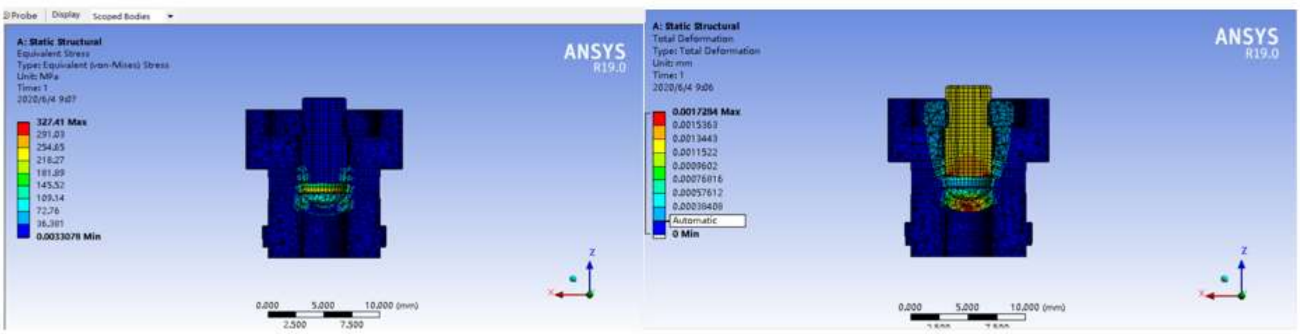

Figure 5. Interference magnitude 0.0028mm sensor stress-strain distribution

ISSN: 2710-0588

3.3.3. Interference Magnitude 0.0038mm Stress Displacement Analysis

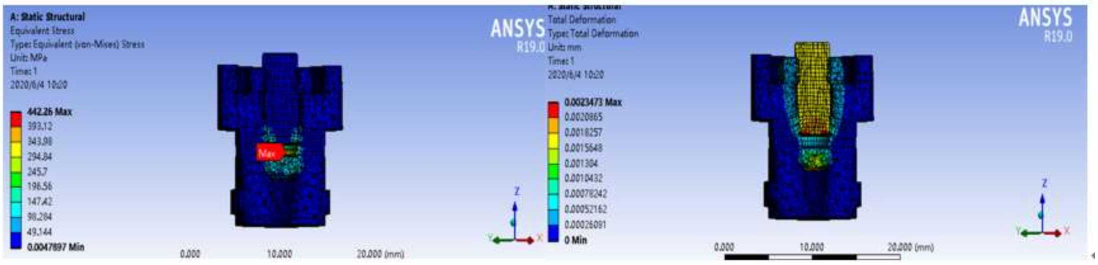

Figure 6. Interference magnitude 0.0038mm sensor stress-strain distribution

3.4. Summary of this Chapter

This chapter analyzes the distribution of stress and strain under three different interference quantities, as shown in the table below. It is concluded that with the increase of preload, the interference quantity also increases, and the maximum stress and strain both increase. However, there is still a distance from the yield limit of the material, so the three cases can work normally, when the interference is 0.0028mm, that is, when the installation torque is 1.5N/m, the effect will be better, which gives a certain reference in the actual installation.

Table 1. Stress and strain under different interference quantities

Magnitude of interference(mm)	Maximum stress (MPa)	maximum strain (mm)	Variable yield limit (MPa)
0.0020	253.13	0.00123	590
0.0028	327.14	0.00173	590
0.0038	442.26	0.00234	590

4. Thermal and Static Performance Analysis of the Sensor under ANSYS

4.1. Temperature Load

4.1.1. Temperature Load Introduction

ANSYS thermal analysis boundary conditions or initial conditions can be divided into seven types:

(1) Temperature: the temperature in the model area is known;

(2) heat flow rate: the point at which the heat flow rate is known;

(3) Convection: heat transfer from the surface to the surrounding fluid through convection. Input convective heat transfer coefficient h and the average temperature of the ambient fluid;

(4) Thermal radiation: the surface through which heat is transmitted. Input radiation coefficient, Stefan-Boltzmann constant, temperature of "space node" as optional input;

(5) adiabatic surface: "completely adiabatic" surface, which does not occur heat transfer;

(6) Heat flux: the surface where the heat flow rate per unit area is known;

(7) Heat generation rate: the area where the heat generation rate of the body is known;

The temperature load is divided into:

① Heat Flow rate.

② Perfectly Insulated.

③ Heat Flux.

4.1.2. Temperature Loading Method

1) Heat Flow rate

ISSN: 2710-0588

Heat flow rate is the amount of heat passing through a heat transfer surface per unit time. Heat exchanger performance is measured by the heat transfer rate, the unit is W. As the concentric load of the node, the heat flow of a point, a side and a surface can be increased; Linear models of objects are usually not directly related to convection and heat flux density.

2) Perfectly Insulated

In order to analyze the plane stresses and axial symmetries in 3D and 2D, fully adiabatic conditions are applied to the surface, which can be considered as the load coefficient of the heat flux in thermal analysis, and if not the load, then in fact the natural boundary conditions.

3) Heat Flux

The density of heat flow refers to the heat entering through the heat transfer area per unit time, that is, under a certain heat flux, the greater the heat flux, the smaller the heat transfer area. Therefore, the heat flux is an evaluation of the heat transfer intensity standard, also known as the heat flux density, the unit is W/m^2 .

4.2. Coupling Analysis of Sensors

4.2.1. Thermoset Coupling Type

As we all know, there are several coupling types of thermos structural coupling: thermal-stress coupling analysis, thermal-electrical coupling analysis, fluid-structure coupling analysis, magneto thermal coupling analysis and magnetic-structure coupling analysis. According to the actual situation and query data, this paper uses the heat-structure coupling method and the heat-structure coupling method to simulate and analyze the high-temperature acceleration piezoelectric sensor, to understand the influence of temperature on the structure, and to analyze the influence of temperature on the structure by analyzing the stress cloud map and strain cloud map of the results. It provides the experimental basis for the optimization design.

4.2.2. Introduction to Thermal - Structural Coupling Analysis

Thermal and structural coupling analysis can be understood as the type of analysis used to analyze the influence of temperature field on physical parameters (such as charge, charge and displacement in the structure), first determine the temperature field to analyze the structure through thermal analysis, then carry out structural analysis, and add the obtained temperature field to the structure as a supporting load to solve the stress distribution of the structure. Thermal structure coupling analysis is now a very basic work of coupling simulation analysis, more and more people like thermal structure coupling analysis, because its analysis steps are very simple, and the results are very accurate.

4.3. Performance Analysis of Sensors at Different Stable Temperatures

4.3.1. Thermal and Structural Coupling Analysis of Sensors At -70℃

Parameters: ambient temperature -70℃, interference amount 0.0028mm, friction coefficient 0.2. The stress-strain diagram is shown in the figure below:

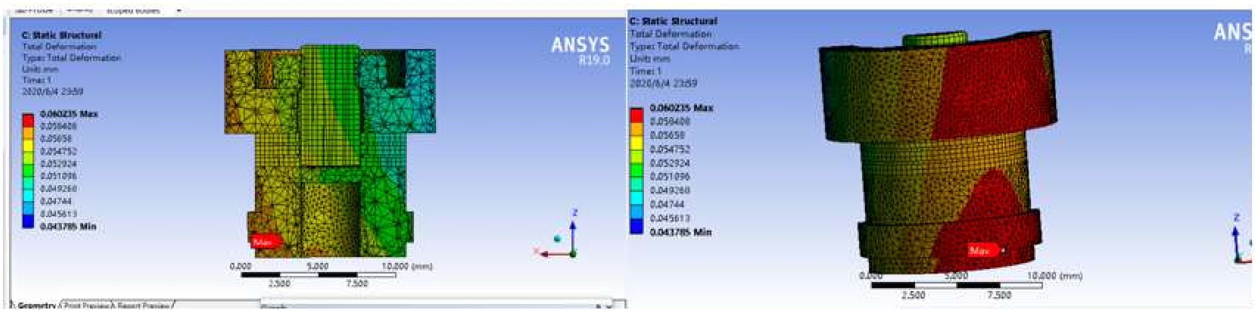

Figure 7. Stress-strain diagram of -70℃ sensor

ISSN: 2710-0588

4.3.2. Thermal and Structural Coupling Analysis of Sensors at -50℃

Parameters: ambient temperature -50℃, interference amount 0.0028mm, friction coefficient 0.2. The stress-strain diagram is shown in the figure below:

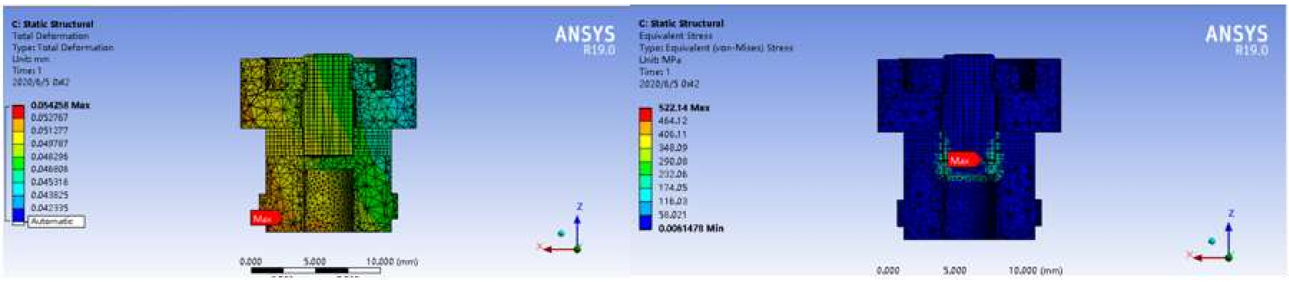

Figure 8. Stress-strain diagram of -50℃ sensor

4.3.3. Thermal and Structural Coupling Analysis of Sensors at 0℃

Parameters: ambient temperature 0℃, interference amount 0.0028mm, friction coefficient 0.2. The stress-strain diagram is shown in the figure below:

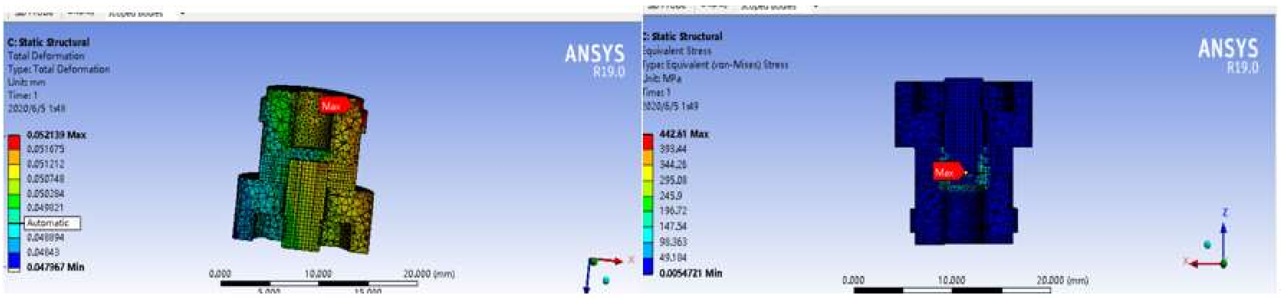

Figure 9. Stress-strain diagram of 0℃ sensor

4.3.4. Thermal and Structural Coupling Analysis of Sensors at 120℃

Parameters: ambient temperature 120℃, interference amount 0.0028mm, friction coefficient 0.2. The stress-strain diagram is shown in the figure below:

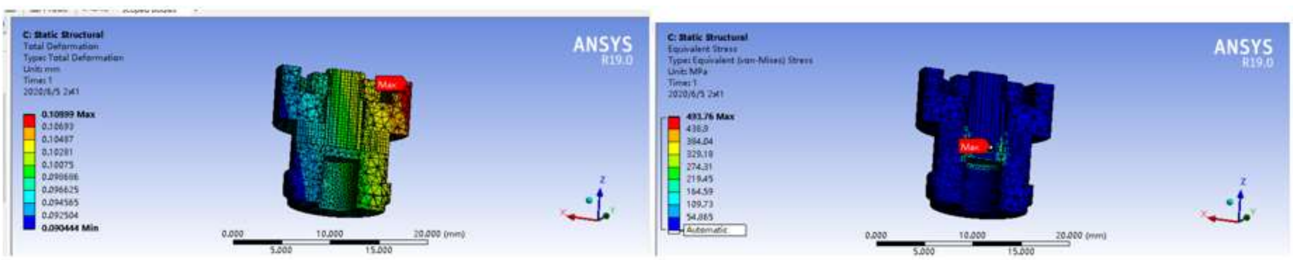

Figure 10. Stress-strain diagram of 120℃ sensor

4.3.5. Thermal and Structural Coupling Analysis of Sensors at 160℃

Parameters: ambient temperature 160℃, interference amount 0.0028mm, friction coefficient 0.2. The stress-strain diagram is shown in the figure below:

ISSN: 2710-0588

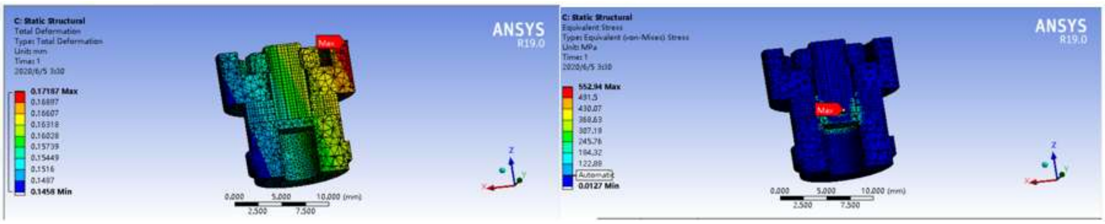

Figure 11. Stress-strain diagram of 160℃ sensor

4.3.6. Thermal and Structural Coupling Analysis of Sensors at 200℃

Parameters: ambient temperature 200℃, interference amount 0.0028mm, friction coefficient 0.2. The stress-strain diagram is shown in the figure below:

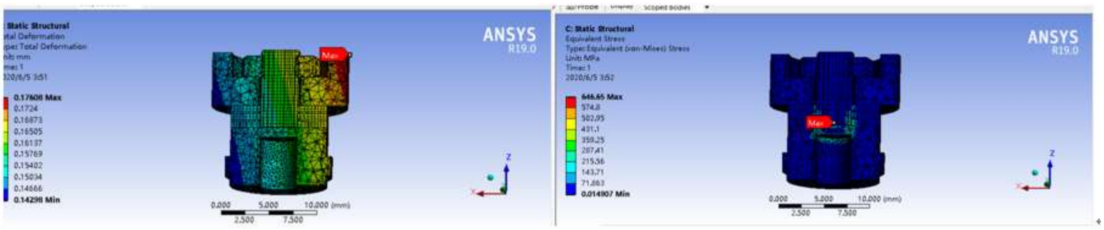

Figure 12. Stress-strain diagram of 200℃ sensor

4.4. Summary of this Chapter

Table 2. Analysis of simulation results under different working conditions

Working condition	Ambient temperature (℃)	Maximum thermal deformation (mm)	Maximum thermal stress (MPa)
1	-70	0.060	579.48
2	-50	0.054	522.14
3	0	0.052	442.61
4	120	0.109	493.76
5	160	0.172	552.94
6	200	0.176	646.65

According to the results of six sets of simulation analysis, as the ambient temperature increases, the thermal stress and strain of the sensor decrease first and then increase. At -70℃, the thermal stress is very close to the yield limit of the material, and at 200℃, the maximum thermal stress has exceeded the yield limit of the material, at which time the structure of the sensor has been damaged and it cannot work normally.

According to the fluid-structure coupling simulation analysis results, the maximum thermal stress of the six working conditions is all on the mass block, among which the maximum is 646.65MPa at 200℃, and when the ambient temperature is 200℃, the thermal deformation is the largest. According to the analysis in the previous section, the stress-strain deformation of the sensor is relatively large at -70℃, 160℃ and 200℃. Therefore, the performance of the sensor will be affected. So we can conclude that the operating temperature of the sensor is between -50℃ and 120℃.

ISSN: 2710-0588

5. Optimal Design of Sensor Structure

5.1. The Principle of Optimal Design

Optimal design is the initial design of a product or element to achieve one of the goals of the design by satisfying the constraints imposed. On this basis, some variable parameters can be modified, so that the generated elements can achieve the best value of the parameters, for example, to optimize the mechanism system, first optimize the mechanism, so that it has enough strength and stiffness to meet the basic needs of the operation, and then try to modify the variable of adjustable parameters, so that the design quality can reach the corresponding minimum goal, which not only reduces the material consumption in the process of manufacturing, but also reduces the quality of the design. It also facilitates the installation of structures. The basic principle of an optimization problem is to express an actual technical problem using mathematical tools, and then solve the problem by implementing an optimization model and obtaining an optimization plan for one or more processes again and again.

5.2. The Thickness of the Sensor Base is Optimized

We know from the previous chapter that the best operating temperature of the sensor is between -50 ° C and 120 ° C. When the temperature is 200℃, the thermal deformation is relatively large, the thermal stress also exceeds the yield strength of the material, and the performance of the sensor will be affected. This chapter will optimize the thickness of the base to see whether the sensor can work normally at 200℃. We studied the thickness of the base of 6.25mm, 6.5mm, 6.75mm, 7mm.

Common scenario parameters: ambient temperature 200℃, interference 0.0028mm. The friction coefficient is 0.2, and the stress-strain distribution is shown in the figure below.

5.2.1. When the Thickness of the Base is 6.25mm

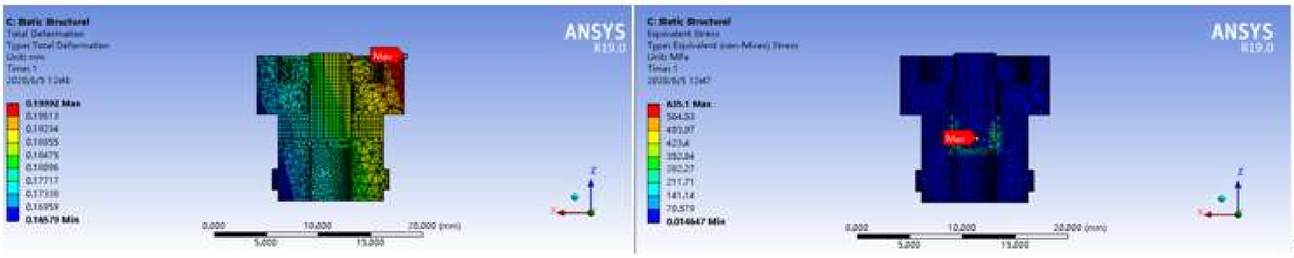

Figure 13. Stress-strain diagram of sensor at thickness of 6.25mm

5.2.2. When the Thickness of the Base is 6.5mm

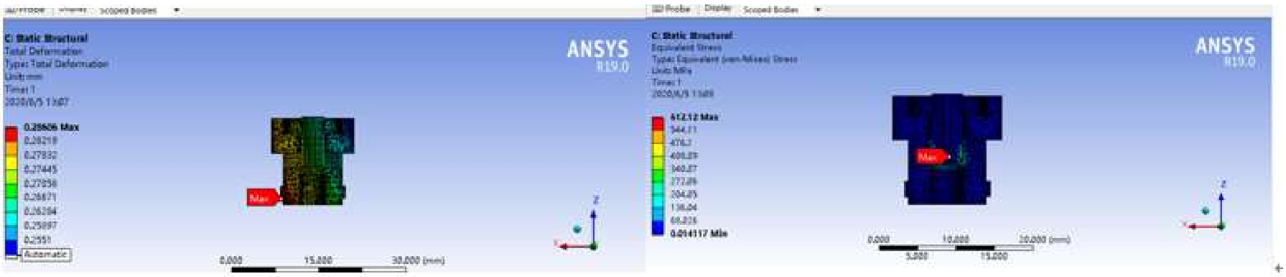

Figure 14. Stress-strain diagram of sensor at thickness of 6.5mm

ISSN: 2710-0588

5.2.3. When the Thickness of the Base is 6.75mm

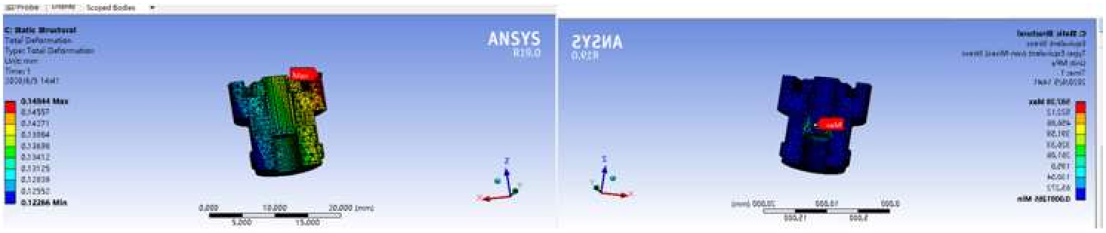

Figure 15. Stress-strain diagram of sensor at thickness of 6.75mm

5.2.4. When the Thickness of the Base is 7mm

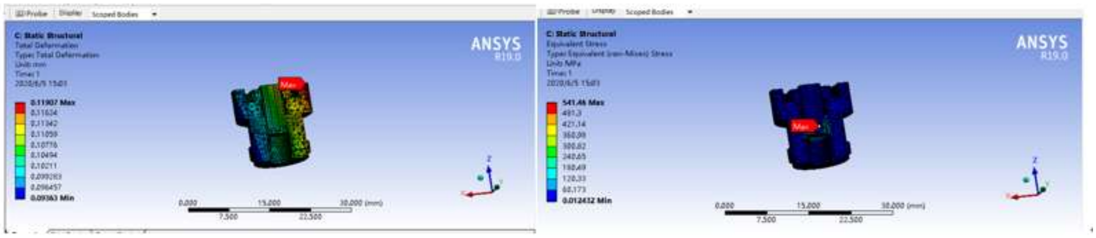

Figure 16. Stress-strain diagram of sensor at thickness of7mm

5.3. Summary Analysis

Table 3. analysis diagram of different diameters

Working condition	Base thickness (mm)	Ambient temperature (℃)	Maximum thermal deformation (mm)	Maximum thermal stress (MPa)
1	6	200	0.176	646.65
2	6.25	200	0.199	635.1
3	6.5	200	0.286	612.12
4	6.75	200	0.148	587.38
5	7	200	0.119	541.46

Base thickness Through the four groups of simulation experiments, compared with the stress-strain under the original size of the base, it is found that with the increase of the thickness of the base, the stress gradually decreases, while the strain increases first and then decreases. When the thickness of the base is 6.25mm and 6.5mm, the thermal stress exceeds the yield strength of the material 590MPa. At this time, the sensor cannot work normally, and the analysis and comparison of the fourth group found that although the stress became much smaller, it was also very close to 590MPa, and the structure of the sensor was relatively relaxed and extremely unstable. When the thickness is increased to 7mm, the thermal deformation and thermal stress are much smaller, and the stress is still some distance from the yield limit of the material, at this time the acceleration sensor can work normally and can adapt to the high temperature environment of 200℃.

6. Conclusion

This paper completed static analysis and thermal analysis of the piezoelectric sensor, and used the interference preload model for analysis. Then, it used the interference preload analysis model to complete thermal analysis at different temperatures, obtained the normal working range of the sensor, and optimized the sensor design. In this paper, the mass block was optimized, and the size of the mass block was increased. Based on the analysis of 0.25mm

ISSN: 2710-0588

spacing, it is concluded that the sensor can work normally at a temperature of 200 when the thickness of the sensor base is 7mm.

The simulation experiment has certain shortcomings, such as low accuracy, certain errors, and more detailed analysis of the sensor. Accurate simulation models and accurate parameters can contribute to the overall optimization of the product, and may even support new product design and manufacturing.

References

[1] K. K. Lv. Research on Design Technology of Large-range high-frequency piezoelectric acceleration Sensor [M]. China Academy of Engineering Physics, 2008.

[2] Y. J. Luo. Modern Piezoelectricity [M]. Beijing: Science Press, 2001.

[3] C. G. Pang. Mechanical behavior and engineering applications of piezoelectric intelligent structures [J]. Advances in Mechanics, 1998, 28(2): 163-172.

[4] J. R. Fu. Mechanics of Heterogeneous Materials [M]. Beijing: Science Press, 2003.

[5] N. H. Deng. Stress Wave Foundation [M]. National Defense Industry Press, 2005.

[6] P. B. Zeng. Vibration measuring instrument [J]. Chinese Journal of Mechanical Mechanics.1976.